

# Crystal structure characterization, Hirshfeld surface analysis, and DFT calculation studies of 1-(6-amino-5-nitronaphthalen-2-yl)ethanone

Xin-Wei Shi,<sup>a</sup> Ming-Sheng Bai,<sup>b</sup> Shao-Jun Zheng,<sup>c</sup> Qiang-Qiang Lu,<sup>a</sup> Gen Li<sup>a</sup> and Ya-Fu Zhou<sup>a\*</sup>

Received 26 February 2024

Accepted 25 April 2024

Edited by A. Briceno, Venezuelan Institute of Scientific Research, Venezuela

**Keywords:** crystal structure; naphthalene ring; Hirshfeld surface analysis; DFT calculations.

**CCDC reference:** 2350991

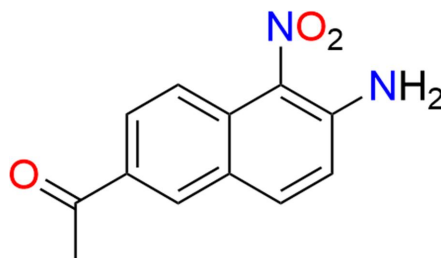
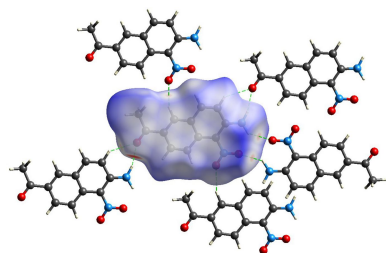
**Supporting information:** this article has supporting information at journals.iucr.org/e

<sup>a</sup>Shaanxi Engineering Research Centre for Conservation and Utilization of Botanical Resources, Xi'an Botanical Garden of Shaanxi Province (Institute of Botany of Shaanxi Province), Xi'an 710061, People's Republic of China, <sup>b</sup>School of Life Sciences, Ningxia University, Yinchuan 750021, People's Republic of China, and <sup>c</sup>School of Environmental and Chemical Engineering, Jiangsu University of Science and Technology, Zhenjiang 212003, People's Republic of China. \*Correspondence e-mail: yafu-zhou@xab.ac.cn

The title compound, C<sub>12</sub>H<sub>10</sub>N<sub>2</sub>O<sub>3</sub>, was obtained by the deacetylation reaction of 1-(6-amino-5-nitronaphthalen-2-yl)ethanone in a concentrated sulfuric acid methanol solution. The molecule comprises a naphthalene ring system bearing an acetyl group (C-3), an amino group (C-7), and a nitro group (C-8). In the crystal, the molecules are assembled into a two-dimensional network by N···H/H···N and O···H/H···O hydrogen-bonding interactions. *n*- $\pi$  and  $\pi$ - $\pi$  stacking interactions are the dominant interactions in the three-dimensional crystal packing. Hirshfeld surface analysis indicates that the most important contributions are from O···H/H···O (34.9%), H···H (33.7%), and C···H/H···C (11.0%) contacts. The energies of the frontier molecular orbitals were computed using density functional theory (DFT) calculations at the B3LYP-D3BJ/def2-TZVP level of theory and the LUMO–HOMO energy gap of the molecule is 3.765 eV.

## 1. Chemical context

2-Naphthylamine (also known as  $\beta$ -naphthylamine, CAS 91-59-8) occurs as pink crystals under the influence of light and has a weak, aromatic odor. In the past, It has been used for ligands or surfactants for the production of azo dyes, as an antioxidant in the rubber industry, as well as in the cable industry (Czubacka *et al.*, 2020). It is also used for oxytocinase assays, water analysis, and sewage control, and as a model bladder carcinogen in laboratories (Freudenthal *et al.*, 1999). It is not currently produced on an industrial scale and is not found in the natural state.



2-Naphthylamine derivatives find applications in organic synthesis and serve as building blocks in the synthesis of dyes (Czubacka *et al.*, 2020), pharmaceuticals (Wu *et al.*, 2024), and other organic compounds (Ding *et al.*, 2005; Yao *et al.*, 2013). The title 2-naphthylamine derivative, (**I**) was obtained by the deacetylation reaction of 2-acetyl-6-acetylamino-5-nitro-

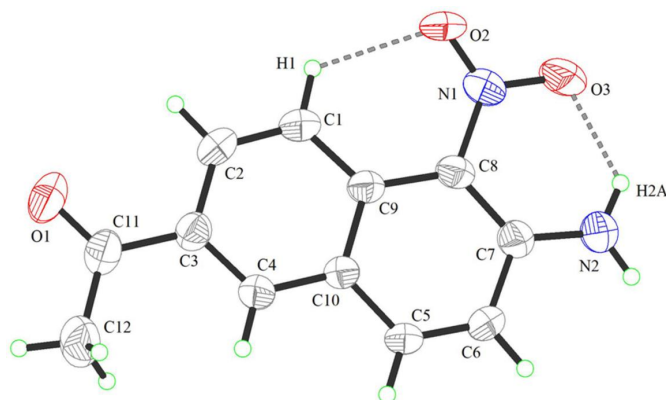


**Figure 1**  
The title molecule atomic numbering scheme. Displacement ellipsoids are depicted at the 50% probability level. The C1–H1···O2 and N2–H2A···O3 intramolecular hydrogen bonds are depicted by gray dashed lines.

naphthalene in concentrated sulfuric acid methanol solution. Herein we report the crystal structure, Hirshfeld surface analysis, and density functional theory (DFT) calculations of the molecule.

## 2. Structural commentary

The title compound (Fig. 1) comprises a naphthalene core structure, where all carbon atoms within the naphthalene ring system (C1–C10) are ideally  $sp^2$ -hybridized. The amino group and the nitro group are adjacent, located at positions C-7 and C-8, respectively, of the naphthalene ring system, while the acetyl group is located at the C-3 position. The angles between the two hydrogen atoms on the amino group and between the two oxygen atoms on the nitro group are 120 and 118.66 (17)°, respectively. The O2–N1–C8–C9 and O2–N1–C8–C7 torsion angles are 112.80 (3) and –165.8 (2)°, respectively. The acetyl group and naphthalene ring system are almost coplanar, the O1–C11–C3–C2 and C12–C11–C3–C4 torsion angles being 2.00 (3) and 2.80 (3)°, respectively. The

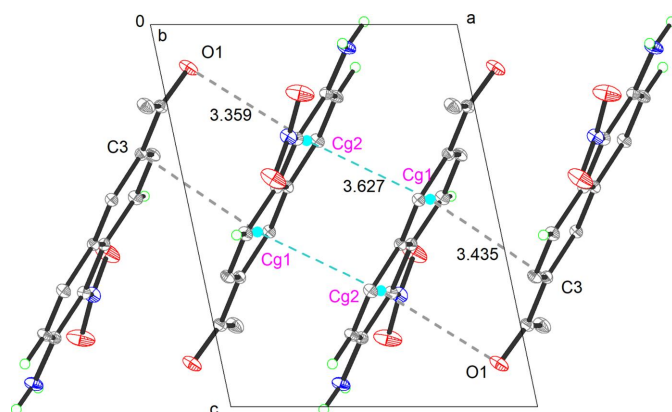


**Figure 2**  
The packing of the molecules showing the  $n$ - $\pi$  and  $\pi$ - $\pi$  stacking interactions (dashed lines) along the  $a$ -axis direction.

**Table 1**  
Hydrogen-bond geometry (Å, °).

$D-H\cdots A$	$D-H$	$H\cdots A$	$D\cdots A$	$D-H\cdots A$
N2–H2B···O1 <sup>i</sup>	0.86	2.16	2.988 (2)	162
N2–H2A···O3 <sup>ii</sup>	0.86	2.54	3.146 (3)	128
N2–H2A···O3	0.86	1.95	2.556 (3)	127
C6–H6···O1 <sup>i</sup>	0.93	2.57	3.341 (2)	141
C1–H1···O2	0.93	2.11	2.720 (3)	122

Symmetry codes: (i)  $x + 1, y, z - 1$ ; (ii)  $-x + 1, -y + 2, -z$ .

intramolecular N2–H2A···O and C1–H1···O2 hydrogen bonds (Table 1) lead to the formation of two six-membered rings, stabilizing the molecular conformation (Fig. 1). The structure of **1** is further stabilized by atom–centroid and centroid–centroid ( $Cg$ – $Cg$ ) interactions, illustrated in Fig. 2.

## 3. Supramolecular features

In the crystal, the molecules are linked *via* C6–H6···O1 and N2–H2B···O1 hydrogen bonds (Table 1), generating two-dimensional layers propagating along the [101] direction (Fig. 3). Two-dimensional layers formed by N2–H2A···O3 intermolecular hydrogen bonds (Fig. 3) while  $n$ - $\pi$  and  $\pi$ - $\pi$  stacking interaction form a super three-dimensional network structure (Fig. 2). The  $\pi$ - $\pi$  interactions are medium-to-weak ( $Cg1$ – $Cg2$  distances greater than 3 Å with a slippage value 3.627 Å where  $Cg1$  and  $Cg2$  are the centroids of the C1–C4/C10/C9 and C5–C10 rings, respectively). In addition, The structure exhibits typical  $n$ - $\pi$  (O1··· $Cg2$  = 3.359 Å) and van der Waals interactions (C3··· $Cg1$  = 3.435 Å).

## 4. Database survey

A survey of the Cambridge Structural Database (CSD version 2024.1.0; Groom *et al.*, 2016) revealed a total of nine compounds with structural similarity greater than 70%, of which six have an acetyl or nitro substituent connected to the naphthalene ring core structure. However, there is only one compound with both acetyl and amino groups on the naphthalene ring system (refcode EBUXIL, CCDC 955350; Rejc *et al.*, 2014).

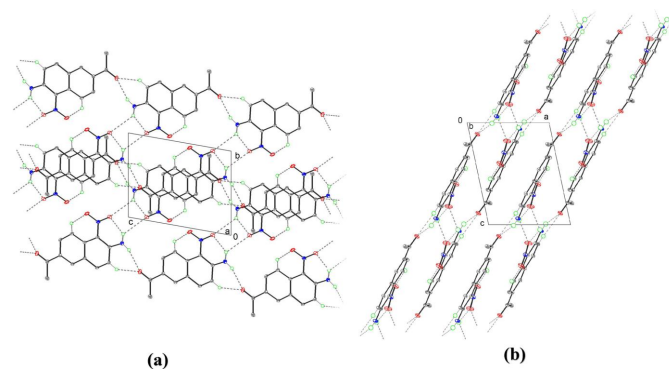


**Figure 3**  
The packing of molecules showing the hydrogen-bonding interactions (gray dashed lines) along (a) the  $a$ -axis direction and (b) the  $b$ -axis direction.

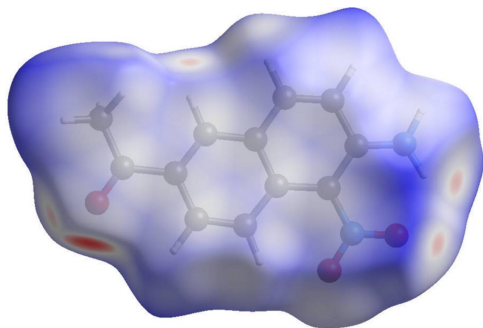


**Figure 4**  
View of the three-dimensional Hirshfeld surface mapped over  $d_{\text{norm}}$ .

## 5. Hirshfeld Surface analysis

In order to visualize the intermolecular interactions, a Hirshfeld surface analysis (Hirshfeld, 1977) was carried out using *Crystal Explorer 21.5* (Spackman *et al.*, 2021). The three-dimensional  $d_{\text{norm}}$  surface of the title compound, plotted with a standardized resolution and color scale ranging from  $-0.4536$  (red) to  $1.4893$  (blue) a.u. is shown in Fig. 4. It reveals the primary interactions to be internal and external hydrogen bonds,  $n-\pi$  and  $\pi-\pi$  interactions. The intense red spots symbolize short contacts and negative  $d_{\text{norm}}$  values on the surface are related to the presence of the  $\text{N2}-\text{H2A}\cdots\text{O3}$  hydrogen bonds in the crystal structure. Weak  $\text{C1}-\text{H1}\cdots\text{O2}$  and  $\text{C6}-\text{H6}\cdots\text{O1}$  contacts are shown by dim red spots (Fig. 5). The 2D fingerprint plots quantitatively visualize the  $\text{H}\cdots\text{O}/\text{O}\cdots\text{H}$ ,  $\text{H}\cdots\text{H}$ ,  $\text{H}\cdots\text{C}/\text{C}\cdots\text{H}$ , and  $\text{H}\cdots\text{N}/\text{N}\cdots\text{H}$  interactions (Fig. 6). The  $n-\pi$  and  $\pi-\pi$  stacking interactions, located in the middle region of the fingerprint plot, play an integral role in the overall crystal packing, contributing 16.6% (Fig. 6a). The most significant contacts are  $\text{H}\cdots\text{O}/\text{O}\cdots\text{H}$  and  $\text{H}\cdots\text{H}$ , contributing 34.9% and 33.7%, respectively, while the  $\text{H}\cdots\text{C}/\text{C}\cdots\text{H}$  contacts contribute 11.0%, and the  $\text{H}\cdots\text{N}/\text{N}\cdots\text{H}$  contacts contribute 3.8% to the Hirshfeld surface (Fig. 6b–6e). The Hirshfeld surfaces mapped over shape-index, curvedness, electrostatic potential, and fragment patches are

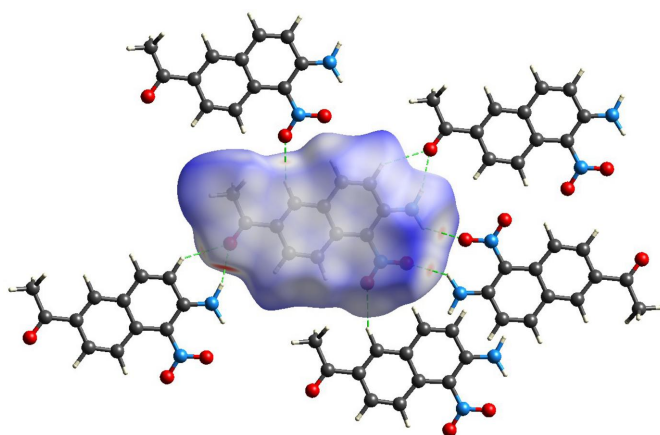


**Figure 5**  
Hirshfeld surface mapped over  $d_{\text{norm}}$  showing  $\text{H}\cdots\text{O}/\text{O}\cdots\text{H}$ ,  $\text{H}\cdots\text{N}/\text{N}\cdots\text{H}$ , and  $\text{C}\cdots\text{H}/\text{H}\cdots\text{C}$  contacts.

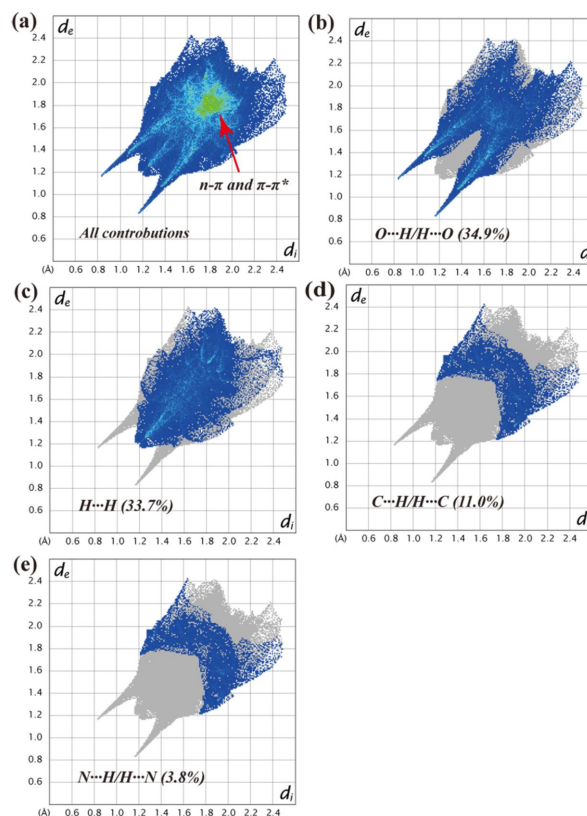


**Figure 6**  
The two-dimensional fingerprint plots showing (a) all interactions, and delineated into (b)  $\text{O}\cdots\text{H}/\text{H}\cdots\text{O}$ , (c)  $\text{H}\cdots\text{H}$ , (d)  $\text{C}\cdots\text{H}/\text{H}\cdots\text{C}$ , and (e)  $\text{N}\cdots\text{H}/\text{H}\cdots\text{N}$  interactions [the  $d_e$  and  $d_i$  values represent the distances (in Å) from a point on the Hirshfeld surface to the nearest atoms inside and outside the surface, respectively].

shown in Fig. 7. The pattern of orange and blue triangles on the shape-index surface (Fig. 7a) shows the characteristic feature of  $\pi-\pi$  interactions. Since curvedness plot (Fig. 7b) shows flat regions, it is evident that the title molecules are arranged in planar stacking (Spackman *et al.*, 2009).

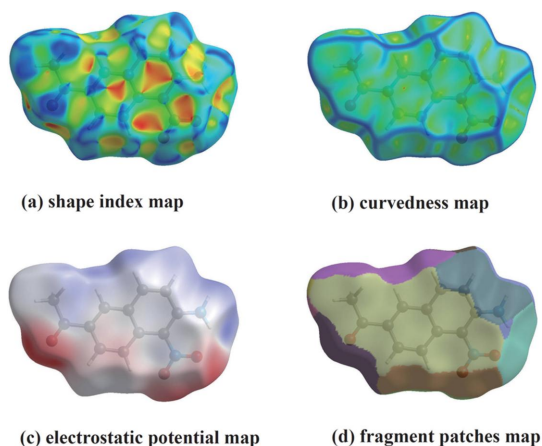


**Figure 7**  
Hirshfeld surfaces mapped over (a) electrostatic potential, (b) shape-index, (c) curvedness, and (d) fragment patches.

**Table 2**

Comparison of selected (X-ray and DFT) geometric data (Å, °).

Bonds/angles	X-ray	$\omega$ B97M-V/def2-TZVP
C12—C11	1.492 (3)	1.514
C10—C4	1.398 (2)	1.406
C11—C3	1.483 (3)	1.491
C10—C5	1.422 (2)	1.419
C11—O1	1.215 (2)	1.215
C5—C6	1.338 (3)	1.354
C3—C2	1.408 (3)	1.410
C6—C7	1.431 (3)	1.427
C3—C4	1.373 (2)	1.378
C7—C8	1.412 (3)	1.410
C2—C1	1.366 (3)	1.371
C7—N2	1.333 (2)	1.348
C1—C9	1.416 (3)	1.418
C8—N1	1.425 (2)	1.446
C9—C10	1.424 (2)	1.427
N1—O2	1.217 (2)	1.223
C9—C8	1.447 (3)	1.437
N1—O3	1.227 (2)	1.240
C3—C11—C12	119.48 (18)	118.71
C5—C10—C9	119.73 (16)	119.45
O1—C11—C12	119.56 (19)	120.66
C3—C4—C10	122.33 (17)	121.48
O1—C11—C3	120.96 (19)	120.63
C6—C5—C10	122.09 (17)	121.61
C2—C3—C11	120.46 (17)	118.95
C5—C6—C7	121.51 (17)	119.00
C4—C3—C11	122.46 (17)	122.97
C8—C7—C6	117.75 (16)	117.98
C4—C3—C2	117.08 (17)	118.02
N2—C7—C6	115.85 (17)	117.13
C1—C2—C3	122.07 (17)	121.89
N2—C7—C8	126.40 (17)	124.87
C2—C1—C9	121.76 (17)	121.22
C7—C8—C9	121.77 (16)	121.48
C1—C9—C10	116.07 (16)	116.84
C7—C8—N1	118.03 (16)	118.18
C1—C9—C8	126.75 (16)	125.24
N1—C8—C9	120.18 (16)	120.31
C10—C9—C8	117.15 (16)	117.85
O2—N1—C8	120.96 (17)	119.41
C4—C10—C9	120.65 (16)	120.53
O2—N1—O3	118.66 (17)	121.99
C4—C10—C5	119.62 (16)	120.01
O3—N1—C8	120.21 (18)	118.58

## 6. DFT calculations

The molecular structure of the title compound in the gas phase was optimized using density functional theory (DFT) (Neese *et al.*, 2009) with the standard B3LYP-D3BJ method with the basis set def2-TZVP (Hanwell *et al.*, 2012), default SCF and geometrical convergence criteria as implemented in the *Orca 5.0.4* package (Neese, 2018, 2022). The input files were prepared from the CIF file using *Avogadro 1.98.1* software (Hanwell *et al.*, 2012). The calculated bond lengths and bond angles for the title compound are presented in Table 2 along with the corresponding crystallographic data (from the CIF file) for comparison. The computed results agree well with the experimental crystallographic data.

Electron distribution in the frontier molecular orbital (FMOs), *i.e.* the highest occupied MO (HOMO;  $-6.357$  eV) and the lowest unoccupied MO (LUMO;  $-2.592$  eV) with a LUMO–HOMO gap of  $3.765$  eV, are illustrated in Fig. 8. The HOMO is less distributed on the naphthyl acetyl group while

**Table 3**

Calculated energies for the title compound.

Molecular energy	Compound (I)
Total energy, $TE$ (eV)	$-21726.75$
$E_{\text{HOMO}}$ (eV)	$-6.357$
$E_{\text{LUMO}}$ (eV)	$-2.592$
Gap, $\Delta E$ (eV)	$3.765$
Dipole moment, $\mu$ (Debye)	$7.33$
Ionization potential, $I$ (eV)	$8.16$
Electron affinity, $A$	$0.77$
Electronegativity, $\chi$	$4.46$
Hardness, $\eta$	$7.40$
Electrophilicity index, $\omega$	$1.34$
Softness, $\sigma$	$0.14$
Fraction of electron transferred, $\Delta N$	$0.69$

LUMO is more distributed. When the energy gap is small, the molecule exhibits high polarizability and enhances its chemical reactivity. The calculated energies and related parameters are presented in Table 3. The hardness and softness values are important parameters in understanding the chemical reactivity of a compound and stability index of a ligand. Compounds formed with a ligand exhibiting higher dipole moment values are generally more stable (Zhan *et al.*, 2003).

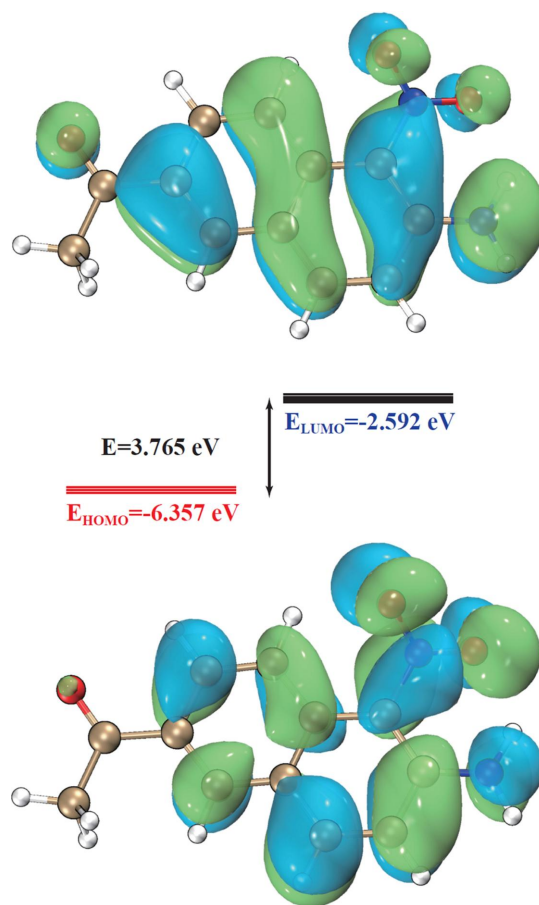


**Figure 8**

HOMO and LUMO calculated by the B3LYP-D3BJ/def2-TZVP method. The energy band gap is shown.

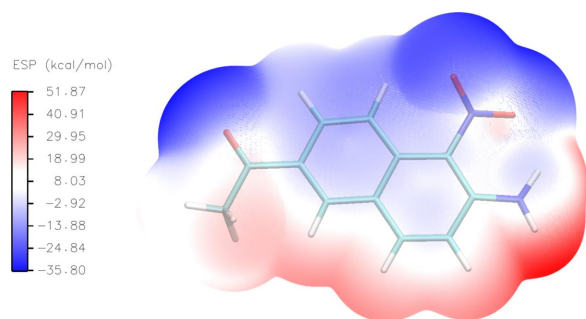


**Figure 9**  
Molecular electrostatic potential (MEP) surfaces mapped from the optimized geometries of the  $\omega$ B97M-V/def2-TZVP calculation.

## 7. Molecular electrostatic potential (MEP)

The molecular electrostatic potential (MEP) map, generated using  $\omega$ B97M-V/def2-TZVP (Mardirossian & Head-Gordon, 2016) basis sets with the *Orca 5.0.4* software package (Neese, 2022), was used to broadly predict reactive sites for electrophilic and nucleophilic attack in the title compound. The map, drawn using *VMD 1.9.4* (Humphrey & Schulten, 1996) and *Multiwfn 3.8* (Lu & Chen, 2012; Zhang & Lu, 2021), is shown in Fig. 9. In the crystal, the molecular charge distribution is governed by the MEP. The electrostatic potential in the MEP map varies increasingly according to a red < white < blue color scheme [ranging from  $-35.80 \text{ kcal mol}^{-1}$  (extreme red) to  $51.87 \text{ kcal mol}^{-1}$  (extreme blue)].

## 8. Synthesis and crystallization

0.5 g of 2-acetyl-6-acetamido-5-nitronaphthalene were dissolved in 30 mL of MeOH, 3 mL of concentrated  $\text{H}_2\text{SO}_4$  was, and the reaction was refluxed at 353 K for 6 h. After the reaction was complete, it was quenched with 10 mL of ice water, precipitating yellow solids, and filtered to obtain the target product. The MeOH was dissolved and red transparent block-shaped crystals were cultured at 277 K in the refrigerator (Xu *et al.*, 2017).

## 9. Refinement

Crystal data, data collection and structure refinement details are summarized in Table 4. H atoms were positioned geometrically (C–H = 0.93–0.96 Å and N–H = 0.86 Å) and refined as riding, with  $U_{\text{iso}}(\text{H}) = 1.2U_{\text{eq}}(\text{N})$  for NH hydrogen atoms or  $1.5U_{\text{eq}}(\text{C-methyl})$ .

## Acknowledgements

The authors thank Nian Zhao, from Hubei Normal University, for the data collection.

## Funding information

Funding for this research was provided by: the Xi'an Science and Technology Plan Project (grant No. 20NYYF0043); the

**Table 4**  
Experimental details.

Crystal data	
Chemical formula	$\text{C}_{12}\text{H}_{10}\text{N}_2\text{O}_3$
$M_r$	230.22
Crystal system, space group	Triclinic, $P\bar{1}$
Temperature (K)	296
$a, b, c$ (Å)	8.1208 (13), 8.2262 (14), 9.5944 (15)
$\alpha, \beta, \gamma$ (°)	73.338 (4), 72.167 (4), 62.966 (4)
$V$ (Å <sup>3</sup> )	535.19 (15)
$Z$	2
Radiation type	Mo $K\alpha$
$\mu$ (mm <sup>-1</sup> )	0.11
Crystal size (mm)	0.40 × 0.30 × 0.15
Data collection	
Diffractometer	Bruker SMART CCD
Absorption correction	Multi-scan <i>SADABS</i> ; Krause <i>et al.</i> , 2015)
No. of measured, independent and observed [ $I > 2\sigma(I)$ ] reflections	3406, 1884, 1448
$R_{\text{int}}$	0.013
$(\sin \theta/\lambda)_{\text{max}}$ (Å <sup>-1</sup> )	0.594
Refinement	
$R[F^2 > 2\sigma(F^2)], wR(F^2), S$	0.051, 0.148, 1.03
No. of reflections	1884
No. of parameters	155
H-atom treatment	H-atom parameters constrained
$\Delta\rho_{\text{max}}, \Delta\rho_{\text{min}}$ (e Å <sup>-3</sup> )	0.41, -0.30

Computer programs: *SMART* and *SAINT* (Bruker, 2002), *SHELXT2014/7* (Sheldrick, 2015a), *SHELXL2014/7* (Sheldrick, 2015b) and *publCIF* (Westrip, 2010).

Key Research and Development Program of Shaanxi (grant No. 2023-YBNY-248 and 2023-YBNY-100); the Xinjiang Production & Construction Corps Key Laboratory of Protection and Utilization of Biological Resources in Tarim Basin (grant No. BRZD2005); the Foundation of Science and Technology in Shaanxi Province (grant No. 2020TD-050); the Key Research and Development Program of China (grant No. 2021YFD1600400).

## References

- Bruker (2002). *SAINT* and *SMART*. Bruker AXS Inc., Madison, Wisconsin, USA.
- Czubacka, E. & Czerczak, S. (2020). *Med. Pr.* **71**, 205–220.
- Ding, K., Li, X., Ji, B., Guo, H. & Kitamura, M. (2005). *Curr. Org. Synth.* **2**, 499–545.
- Freudenthal, R. I., Stephens, E. & Anderson, D. P. (1999). *Int. J. Toxicol.* **18**, 353–359.
- Groom, C. R., Bruno, I. J., Lightfoot, M. P. & Ward, S. C. (2016). *Acta Cryst.* **B72**, 171–179.
- Hanwell, M. D., Curtis, D. E., Lonie, D. C., Vandermeersch, T., Zurek, E. & Hutchison, G. R. (2012). *J. Cheminf.* **4**, 1–17.
- Hirshfeld, F. L. (1977). *Theor. Chim. Acta*, **44**, 129–138.
- Humphrey, W., Dalke, A. & Schulten, K. (1996). *J. Mol. Graph.* **14**, 33–38.
- Krause, L., Herbst-Irmer, R., Sheldrick, G. M. & Stalke, D. (2015). *J. Appl. Cryst.* **48**, 3–10.
- Lu, T. & Chen, F. (2012). *J. Comput. Chem.* **33**, 580–592.
- Mardirossian, N. & Head-Gordon, M. (2016). *J. Chem. Phys.* **144**, 214110.
- Neese, F. (2018). *Wiley Interdiscip. Rev.: Comput. Mol. Sci.* **8**, e1327.
- Neese, F. (2022). *Wiley Interdiscip. Rev.: Comput. Mol. Sci.* **12**, e1606.

- Neese, F., Wennmohs, F., Hansen, A. & Becker, U. (2009). *Chem. Phys.* **356**, 98–109.
- Rejc, L., Fabris, J., Adrović, A., Kasunić, M. & Petrič, A. (2014). *Tetrahedron Lett.* **55**, 1218–1221.
- Sheldrick, G. M. (2015a). *Acta Cryst.* **A71**, 3–8.
- Sheldrick, G. M. (2015b). *Acta Cryst.* **C71**, 3–8.
- Spackman, M. A. & Jayatilaka, D. (2009). *CrystEngComm*, **11**, 19–32.
- Spackman, P. R., Turner, M. J., McKinnon, J. J., Wolff, S. K., Grimwood, D. J., Jayatilaka, D. & Spackman, M. A. (2021). *J. Appl. Cryst.* **54**, 1006–1011.
- Westrip, S. P. (2010). *J. Appl. Cryst.* **43**, 920–925.
- Wu, J., Liu, X., Zhang, J., Yao, J., Cui, X., Tang, Y., Xi, Z., Han, M., Tian, H., Chen, Y., Fan, Q., Li, W. & Kong, D. (2024). *Bioorg. Chem.* **142**, 106930.
- Xu, Z., Zheng, S. & Liu, Y. (2017). China patent, CN106866437 A.
- Yao, W., Yan, Y., Xue, L., Zhang, C., Li, G., Zheng, Q., Zhao, Y., Jiang, H. & Yao, J. (2013). *Angew. Chem. Int. Ed.* **52**, 8713–8717.
- Zhan, C. G., Nichols, J. A. & Dixon, D. A. (2003). *J. Phys. Chem. A*, **107**, 4184–4195.
- Zhang, J. & Lu, T. (2021). *Phys. Chem. Chem. Phys.* **23**, 20323–20328.

## supporting information

*Acta Cryst.* (2024). E80 [https://doi.org/10.1107/S2056989024003797]

## Crystal structure characterization, Hirshfeld surface analysis, and DFT calculation studies of 1-(6-amino-5-nitronaphthalen-2-yl)ethanone

Xin-Wei Shi, Ming-Sheng Bai, Shao-Jun Zheng, Qiang-Qiang Lu, Gen Li and Ya-Fu Zhou

### Computing details

#### 1-(6-Amino-5-nitronaphthalen-2-yl)ethanone

##### Crystal data

$C_{12}H_{10}N_2O_3$

$M_r = 230.22$

Triclinic,  $P\bar{1}$

$a = 8.1208$  (13) Å

$b = 8.2262$  (14) Å

$c = 9.5944$  (15) Å

$\alpha = 73.338$  (4)°

$\beta = 72.167$  (4)°

$\gamma = 62.966$  (4)°

$V = 535.19$  (15) Å<sup>3</sup>

$Z = 2$

$F(000) = 240$

$D_x = 1.429$  Mg m<sup>-3</sup>

Mo  $K\alpha$  radiation,  $\lambda = 0.71073$  Å

Cell parameters from 1265 reflections

$\theta = 2.8$ – $25.0$ °

$\mu = 0.11$  mm<sup>-1</sup>

$T = 296$  K

Block, red

$0.40 \times 0.30 \times 0.15$  mm

##### Data collection

Bruker SMART CCD

diffractometer

phi and  $\omega$  scans

Absorption correction: multi-scan

SADABS; Krause *et al.*, 2015)

3406 measured reflections

1884 independent reflections

1448 reflections with  $I > 2\sigma(I)$

$R_{int} = 0.013$

$\theta_{max} = 25.0$ °,  $\theta_{min} = 2.3$ °

$h = -9 \rightarrow 9$

$k = -6 \rightarrow 9$

$l = -11 \rightarrow 11$

##### Refinement

Refinement on  $F^2$

Least-squares matrix: full

$R[F^2 > 2\sigma(F^2)] = 0.051$

$wR(F^2) = 0.148$

$S = 1.03$

1884 reflections

155 parameters

0 restraints

Hydrogen site location: inferred from neighbouring sites

H-atom parameters constrained

$w = 1/[\sigma^2(F_o^2) + (0.0735P)^2 + 0.2098P]$

where  $P = (F_o^2 + 2F_c^2)/3$

$(\Delta/\sigma)_{max} < 0.001$

$\Delta\rho_{max} = 0.41$  e Å<sup>-3</sup>

$\Delta\rho_{min} = -0.30$  e Å<sup>-3</sup>

##### Special details

**Geometry.** All esds (except the esd in the dihedral angle between two l.s. planes) are estimated using the full covariance matrix. The cell esds are taken into account individually in the estimation of esds in distances, angles and torsion angles; correlations between esds in cell parameters are only used when they are defined by crystal symmetry. An approximate (isotropic) treatment of cell esds is used for estimating esds involving l.s. planes.

Fractional atomic coordinates and isotropic or equivalent isotropic displacement parameters ( $\text{\AA}^2$ )

	<i>x</i>	<i>y</i>	<i>z</i>	$U_{\text{iso}}^*/U_{\text{eq}}$
C12	0.0695 (3)	0.0991 (3)	0.7872 (3)	0.0632 (7)
H12A	0.1914	0.0236	0.8117	0.095*
H12B	0.0717	0.0847	0.6908	0.095*
H12C	-0.0238	0.0615	0.8599	0.095*
C11	0.0216 (3)	0.2974 (3)	0.7860 (2)	0.0456 (5)
C3	0.1180 (3)	0.3996 (3)	0.6612 (2)	0.0372 (4)
C2	0.0793 (3)	0.5851 (3)	0.6600 (2)	0.0444 (5)
H2	-0.0081	0.6426	0.7383	0.053*
C1	0.1661 (3)	0.6831 (3)	0.5474 (2)	0.0423 (5)
H1	0.1366	0.8052	0.5514	0.051*
C9	0.2999 (2)	0.6039 (2)	0.4247 (2)	0.0324 (4)
C10	0.3356 (2)	0.4177 (2)	0.42440 (19)	0.0328 (4)
C4	0.2454 (3)	0.3209 (2)	0.5420 (2)	0.0357 (4)
H4	0.2726	0.1990	0.5396	0.043*
C5	0.4643 (3)	0.3292 (2)	0.3033 (2)	0.0392 (5)
H5	0.4859	0.2079	0.3040	0.047*
C6	0.5553 (3)	0.4150 (3)	0.1883 (2)	0.0408 (5)
H6	0.6395	0.3514	0.1120	0.049*
C7	0.5262 (3)	0.6024 (3)	0.1800 (2)	0.0380 (5)
C8	0.3990 (3)	0.6942 (2)	0.2985 (2)	0.0357 (4)
N1	0.3732 (3)	0.8791 (2)	0.2929 (2)	0.0489 (5)
N2	0.6247 (3)	0.6726 (3)	0.05977 (18)	0.0538 (5)
H2A	0.6136	0.7843	0.0491	0.065*
H2B	0.6992	0.6062	-0.0071	0.065*
O1	-0.0958 (2)	0.3728 (2)	0.88712 (17)	0.0677 (5)
O2	0.2953 (3)	0.9525 (2)	0.4026 (2)	0.0887 (7)
O3	0.4405 (4)	0.9628 (2)	0.1795 (2)	0.0975 (8)

Atomic displacement parameters ( $\text{\AA}^2$ )

	$U^{11}$	$U^{22}$	$U^{33}$	$U^{12}$	$U^{13}$	$U^{23}$
C12	0.0646 (15)	0.0471 (13)	0.0580 (14)	-0.0232 (12)	0.0059 (11)	0.0006 (11)
C11	0.0401 (11)	0.0489 (12)	0.0382 (10)	-0.0153 (9)	-0.0010 (9)	-0.0056 (9)
C3	0.0336 (9)	0.0373 (10)	0.0363 (10)	-0.0123 (8)	-0.0038 (8)	-0.0075 (8)
C2	0.0427 (11)	0.0456 (11)	0.0397 (10)	-0.0137 (9)	0.0033 (8)	-0.0196 (9)
C1	0.0473 (11)	0.0309 (10)	0.0467 (11)	-0.0133 (9)	-0.0025 (9)	-0.0156 (8)
C9	0.0331 (9)	0.0280 (9)	0.0359 (10)	-0.0104 (7)	-0.0072 (8)	-0.0086 (7)
C10	0.0334 (9)	0.0293 (9)	0.0357 (9)	-0.0120 (8)	-0.0039 (7)	-0.0100 (7)
C4	0.0366 (10)	0.0301 (9)	0.0389 (10)	-0.0137 (8)	-0.0037 (8)	-0.0078 (8)
C5	0.0437 (11)	0.0283 (9)	0.0437 (11)	-0.0145 (8)	0.0003 (8)	-0.0135 (8)
C6	0.0449 (11)	0.0371 (10)	0.0372 (10)	-0.0160 (9)	0.0036 (8)	-0.0154 (8)
C7	0.0427 (11)	0.0361 (10)	0.0357 (10)	-0.0186 (9)	-0.0058 (8)	-0.0049 (8)
C8	0.0409 (10)	0.0271 (9)	0.0399 (10)	-0.0139 (8)	-0.0078 (8)	-0.0072 (8)
N1	0.0591 (11)	0.0313 (9)	0.0543 (11)	-0.0213 (8)	-0.0023 (8)	-0.0092 (8)
N2	0.0723 (13)	0.0476 (10)	0.0405 (10)	-0.0344 (10)	0.0068 (9)	-0.0083 (8)



O1	0.0671 (11)	0.0683 (11)	0.0509 (9)	-0.0280 (9)	0.0205 (8)	-0.0200 (8)
O2	0.1203 (16)	0.0512 (10)	0.0912 (14)	-0.0504 (11)	0.0344 (12)	-0.0407 (10)
O3	0.174 (2)	0.0506 (11)	0.0627 (11)	-0.0669 (13)	0.0141 (12)	-0.0071 (9)

*Geometric parameters (Å, °)*

C12—C11	1.492 (3)	C10—C4	1.398 (2)
C11—O1	1.215 (2)	C10—C5	1.422 (2)
C11—C3	1.483 (3)	C5—C6	1.338 (3)
C3—C4	1.373 (2)	C6—C7	1.431 (3)
C3—C2	1.408 (3)	C7—N2	1.333 (2)
C2—C1	1.366 (3)	C7—C8	1.412 (3)
C1—C9	1.416 (3)	C8—N1	1.425 (2)
C9—C10	1.424 (2)	N1—O2	1.217 (2)
C9—C8	1.447 (3)	N1—O3	1.227 (2)
O1—C11—C3	120.96 (19)	C5—C10—C9	119.73 (16)
O1—C11—C12	119.56 (19)	C3—C4—C10	122.33 (17)
C3—C11—C12	119.48 (18)	C6—C5—C10	122.09 (17)
C4—C3—C2	117.08 (17)	C5—C6—C7	121.51 (17)
C4—C3—C11	122.46 (17)	N2—C7—C8	126.40 (17)
C2—C3—C11	120.46 (17)	N2—C7—C6	115.85 (17)
C1—C2—C3	122.07 (17)	C8—C7—C6	117.75 (16)
C2—C1—C9	121.76 (17)	C7—C8—N1	118.03 (16)
C1—C9—C10	116.07 (16)	C7—C8—C9	121.77 (16)
C1—C9—C8	126.75 (16)	N1—C8—C9	120.18 (16)
C10—C9—C8	117.15 (16)	O2—N1—O3	118.66 (17)
C4—C10—C5	119.62 (16)	O2—N1—C8	120.96 (17)
C4—C10—C9	120.65 (16)	O3—N1—C8	120.21 (18)
O1—C11—C3—C4	-177.21 (19)	C4—C10—C5—C6	-179.61 (18)
C12—C11—C3—C4	2.8 (3)	C9—C10—C5—C6	0.4 (3)
O1—C11—C3—C2	2.0 (3)	C10—C5—C6—C7	-0.8 (3)
C12—C11—C3—C2	-178.01 (19)	C5—C6—C7—N2	-179.82 (18)
C4—C3—C2—C1	-1.1 (3)	C5—C6—C7—C8	0.6 (3)
C11—C3—C2—C1	179.64 (18)	N2—C7—C8—N1	-1.2 (3)
C3—C2—C1—C9	0.2 (3)	C6—C7—C8—N1	178.35 (17)
C2—C1—C9—C10	1.1 (3)	N2—C7—C8—C9	-179.66 (18)
C2—C1—C9—C8	179.23 (18)	C6—C7—C8—C9	-0.2 (3)
C1—C9—C10—C4	-1.7 (3)	C1—C9—C8—C7	-178.23 (18)
C8—C9—C10—C4	-179.93 (16)	C10—C9—C8—C7	-0.2 (3)
C1—C9—C10—C5	178.33 (16)	C1—C9—C8—N1	3.3 (3)
C8—C9—C10—C5	0.1 (3)	C10—C9—C8—N1	-178.64 (16)
C2—C3—C4—C10	0.6 (3)	C7—C8—N1—O2	-165.8 (2)
C11—C3—C4—C10	179.81 (17)	C9—C8—N1—O2	12.8 (3)
C5—C10—C4—C3	-179.17 (17)	C7—C8—N1—O3	9.4 (3)
C9—C10—C4—C3	0.8 (3)	C9—C8—N1—O3	-172.1 (2)

*Hydrogen-bond geometry (Å, °)*

<i>D</i> —H··· <i>A</i>	<i>D</i> —H	H··· <i>A</i>	<i>D</i> ··· <i>A</i>	<i>D</i> —H··· <i>A</i>
N2—H2B···O1 <sup>i</sup>	0.86	2.16	2.988 (2)	162
N2—H2A···O3 <sup>ii</sup>	0.86	2.54	3.146 (3)	128
N2—H2A···O3	0.86	1.95	2.556 (3)	127
C6—H6···O1 <sup>i</sup>	0.93	2.57	3.341 (2)	141
C1—H1···O2	0.93	2.11	2.720 (3)	122

Symmetry codes: (i)  $x+1, y, z-1$ ; (ii)  $-x+1, -y+2, -z$ .